RESEARCH ARTICLE

Spatial distribution of heavy metal contamination and uncertainty-based human health risk in the aquatic environment using multivariate statistical method

Jing Li[2,1] · Yizhong Chen[3] · Hongwei Lu[1] · Weiyao Zhai[2]

Abstract

Heavy metal contamination in the aquatic environment is one of the most serious health issues worldwide. In this study, an evaluation framework is developed to identify the sources and health risk of heavy metals (i.e., As, Hg, Cr, Cu, Zn, Pb, and Cd) contamination in the North Canal of Fengtai District, China, which is based on multiple approaches, including multivariate statistical method, health risk assessment, and uncertainty analysis. Spatial distribution of these heavy metals could exhibit their impact on the aquatic environment. Pearson's correlation analysis shows that a majority of the correlations between different heavy metals are not significant due to the differences in sources of heavy metals. Principal component analysis indicates that there are four principal components to explain 91.381% of the total variance. Moreover, health risk reveals that hazard quotient values are in low levels, ranging from 0.48 to 0.74, relative higher quotient levels could be observed in the northern section. The carcinogenic risk of Cd has exceeded the acceptable level in S1, S3, and S7. Sensitivity analysis ensures the reliability of health risk assessments. Furthermore, some specific recommendations are given to help decision-makers develop more comprehensive strategies for improving water environment quality.

Keywords Heavy metals · Health risk · Multivariate statistical method · Uncertainty analysis · Decision-makers

Introduction

Heavy metal (HM) contamination, especially in the aquatic environment, is one of the most serious health issues worldwide, mainly because of their anthropogenic inputs (De Silva et al.

✉ Yizhong Chen
2019075@hebut.edu.cn

✉ Hongwei Lu
luhw@igsnrr.ac.cn

1   Key Laboratory of Water Cycle and Related Land Surface Processes, Institute of Geographic Science and Natural Resources Research, Chinese Academy of Sciences, Beijing 100101, China

2   Hebei Key Laboratory of Environmental Change and Ecological Construction, Hebei Technology Innovation Center for Remote Sensing Identification of Environmental Change, College of Resources and Environmental Sciences, Hebei Normal University, Shijiazhuang 050024, China

3   School of Economics and Management, Hebei University of Technology, Tianjin 300401, China

2015; Deepa and Jitendra 2019; Islam et al. 2020b). HMs frequently accumulate in sediments, and they cannot easily be removed by biodegradation or chemical degradation (Bartoli et al. 2012; Haris et al. 2017; Hossain et al. 2019; Haghshenas et al. 2019; Hosseini et al. 2020). The sources of HMs in the aquatic environment are natural and anthropogenic activities, such as agriculture runoff, unfettered industrialization, rapid urbanization, and massive use of fossil fuels (Zafra et al. 2017). It should be specifically mentioned that HMs, like mercury (Hg), arsenic (As), copper (Cu), chromium (Cr), lead (Pb), zinc (Zn), and cadmium (Cd), are of a high concern since they have direct impacts on human health through affecting the food chains (Martinez-Cortijo and Ruiz-Canales 2018; Paschoalini et al. 2019). Exposure to these HMs, dermal absorption, inhalation, and direct intake could result in serious diseases, such as hypertension, renal dysfunction, and cancer (Saha et al. 2017; Devi and Yadav 2018; Tepanosyan et al. 2018). Hence, analyzing the sources, spatial distribution patterns, and health risks of HMs in the aquatic environment is an important undertaking (Swain and Sahoo 2017).

Currently, the level of HM contamination in the aquatic environment and the related risks have received considerable

attention, and multiple approaches have been applied for their assessment (Nath et al. 2018; Pal and Maiti 2018; Withanachchi et al. 2018; Zivkovic et al. 2019;). Excess abundances of As in shellfish was detected in the Pearl River Delta in South China (Yu et al. 2021). Copper, zinc, and iron were widely detected in the Dawen River basin of Shandong Province in China, followed by nickel, arsenic, selenium, lead, and mercury (Liu et al. 2021). Among these researches, the widely used analysis techniques for metal contamination based on existing water quality standards are the heavy metal pollution index (HPI) and pollution index (PI). These simple approaches facilitate the analysis of pollution sources and the verification of protection measures based on generated solutions (Zhang et al. 2017). According to the U.S. Environmental Protection Agency (USEPA), the evaluation of potential health risks and the spatial distribution of HMs should be conducted to identify carcinogenic and non-carcinogenic risks. For example, Singh and Kumar (2017) focused on HM contamination in the Ajay River with consideration of seasonal and spatial variations by analyzing 76 samples for 2 years. Results showed that the mean values of HPI and PI were found above the critical index owing to a higher concentration of Cd, Pb, and Fe. Solutions of health risk assessment disclosed that high loads of Cd, Pb, and Fe in the surface water could harm the population. Islam et al. (2020a) analyzed concentrations of eight trace elements in surface water in Bangladesh. Six assessment methods were used to evaluate the water quality and health risks, including hazard index and Monte Carlo simulation. Results showed that the values of the hazard index surpassed the acceptable level. Carcinogenic risks of Cr also exceeded the acceptable level for adults and children. Habib et al. (2020) appraised 10 trace metals in groundwater samples using multivariate statistical approaches, health risk model, and Monte Carlo simulation. Results of hazard index evaluation showed the values exceeded the safe levels for adults and children. The carcinogenic risk values of Cd and Cr exceeded acceptable levels as well, with oral intake as the key exposure pathway.

Although existing efforts have helped identify the associated health risks of HM contamination in the aquatic environment, much needs to be done with regard to the uncertainties arising from modeling parameters, such as pollutant concentration, carcinogenic slope factors, and daily ingestion (Keller et al. 2002; Albuquerque et al. 2017; Troldborg et al. 2017; Eze et al. 2019; Shabanda et al. 2019). The lack of consideration for uncertain information could cause the obtained solutions to deviate from the "true" solutions of identified problems (Harris et al. 2017; Sharafi et al. 2019). Uncertainties expressed as probability distributions have been widely investigated, and the results could provide decision-makers with multiple optimal strategies under different probability levels. However, in the general decision-making process, difficulties arise when tackling cumbersome water quality datasets. Multiple statistical analyses, e.g.,

principal component analysis (PCA) and cluster analysis (CA), provide a powerful approach for classifying, modeling, and interpreting complex water quality datasets (Astel et al. 2007; Peiris et al. 2010; Maere et al. 2012; Viswanath et al. 2015; Javadi et al. 2017). In water quality evaluation, identifying the interrelations in huge datasets, and the key factors greatly affecting the aquatic environment is critical. Accordingly, PCA should be applied to process water quality datasets so as to identify the hypothetical sources of HMs, minimizing the number of variables with high loadings on each component. CA can classify these samples with similar HM contents. Specifically, R-mode CA could evaluate the association between various parameters and sources of water quality while Q-mode CA is used to determine similar site clusters (Bayo and López-Castellanos 2016; Delpal et al. 2018).

The purpose of this study is to establish evaluation methods for identifying the degree of contamination and health risk of HMs in the aquatic environment. Seven HMs (Pb, As, Cr, Cd, Cu, Hg, and Zn) will be considered to compute the exposure rates of HMs for human health through ingestion owing to their toxic properties. Spatial distribution of these HMs will be presented to exhibit the impact of contaminants on the aquatic environment. Additionally, multiple statistical analysis is used to determinate the connection between different HM contamination.

Materials and methods

Overview of the study region

This study focuses on the North Canal of Fengtai District (from 39 45′ to 39 55′ N in latitude, and from 116 03′ to 116 30′ E in longitude), which is located along the western border of Beijing, China (Fig. 1). This district has an area of 205.87 km² and 2.26 million of the population (Chen et al. 2016). In terms of the geological and geomorphology, there are different geological conditions in the western and eastern parts of Fengtai District, where stratigraphic lithology in different geologic time is distributed. The western and eastern parts are respectively composed of mountains and plains. The soil types in Fengtai District are mainly brown and tidal soils, which account for 67% and 29% of the soil in the whole region, respectively, while the rest are mostly composed of wind sand and paddy soils. Among them, the brown soil is mainly distributed in the western, northern, southeastern parts of the region, and the tidal soil is principally located in the middle and southern parts. When it comes to the meteorological and hydrological conditions, this district is a typical continental and semi-arid climate of a warm temperate zone. The annual average temperature is 11.7 °C, and the annual average precipitation is 580.6 mm. The average annual surface evaporation is 934.7 mm, and the land evaporation is about 472.2 mm.
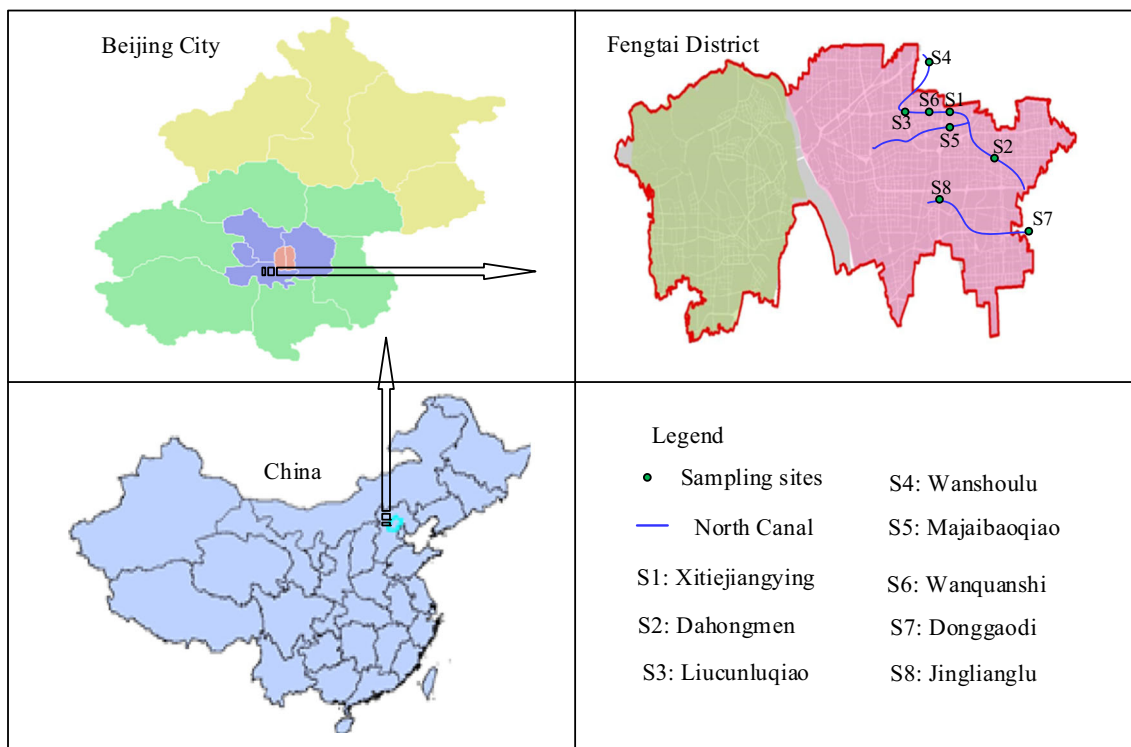
Fig. 1 Schematic of the aquatic environment in Fengtai district, Beijing, China

In addition, there are three major rivers in this district, namely the Yongding River, North Canal, and Daqing River. Because of insufficient water in the Yongding River and Daqing River for many years, this study centers mostly on the North Canal, which has a length of 68 km (8.8 km in Fengtai District) and a basin area of 630 km^2. With rapid development of economy and continued acceleration of the population, the increasingly severe water contamination has become one of the trickiest problems. For example, rivers with grade V accounted for more than 95% of all rivers in 2013, and according to Fengtai District environmental quality report in 2012, the super standard rate of chemical oxygen demand (COD), potassium permanganate index (PPI), biological oxygen demand (BOD), ammonia nitrogen (NH$_3$-N), and total phosphorus (TP) were examined up to 67.4%, 37.5%, 87.5%, 85.9%, and 100%, respectively (Fig. 2) (Chen et al. 2017). The study area belongs to a warm temperate semi-arid and semi-humid continental monsoon climate. The annual average temperature is 11~12 °C, the annual average precipitation is 551.9 mm, and more than 85% of the annual rainfall is concentrated in June to September. The study area is located in the alluvial proluvial plain of Chaobai River, with a Quaternary sedimentary thickness of more than 300 m. the lithology is mainly composed of interbedding of silty clay, silty sand, and fine sand. In this study, eight sampling sites have been used to determine its water contaminations (Fig. 1). All of the eight sampling sites are on the North Canal. The monitoring sites are established by the government of Fengtai District, and the water quality is regularly monitored by the Beijing Municipal Ecology and Environment Bureau.

Multivariate statistical analysis

Principal component analysis aims to turn multiple index problems into a few comprehensive variables with less information loss, which could significantly improve the efficiency of analysis. According to the sample attributes, a hierarchical clustering method set is introduced to cluster the network nodes. In this study, R software and SPSS software are applied to reduce the dimension of seven HMs based on PCA and to analyze the correction and primary sources of pollutants. Moreover, these seven HMs are classified by cluster analysis, the HMs with similar attributes or sources are then obtained, and such results could be further verified by a PCA approach.

Human health risk assessment

It is increasingly desired to identify the probability of carcinogenic and non-carcinogenic risks to a human body owing to HMs in the aquatic environment (USEPA 2000; Lu et al. 2018). There are two major exposure pathways, i.e., dermal contact absorption and direct ingestion. In this study, only direct ingestion is considered due to its higher environmental risks. The chronic daily intake (CDI), hazard quotient (HQ), and hazard index are calculated according to USEPA standards, which could determinate the ingestion rate of contamination.

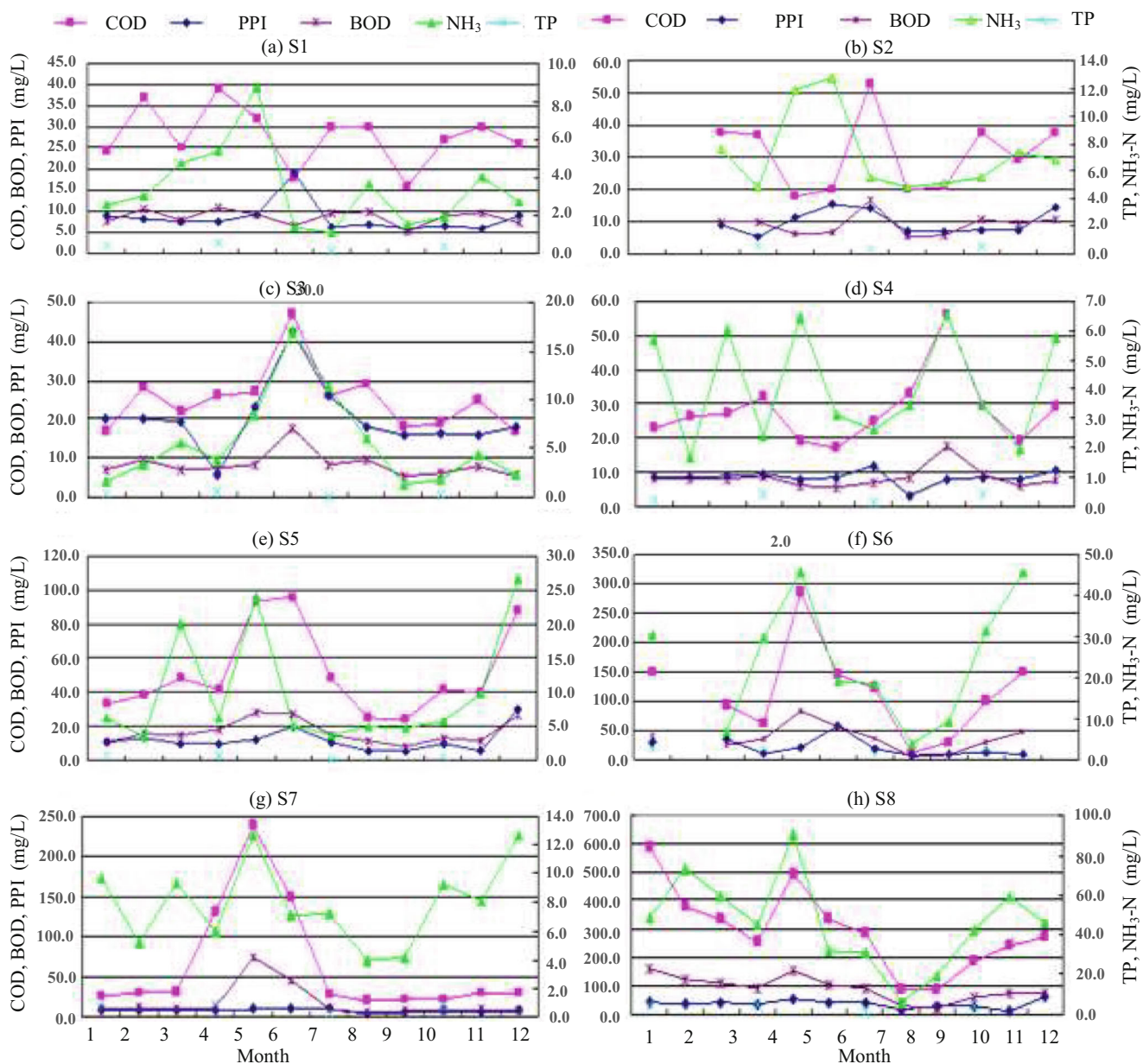$$CDI_i = \frac{EC_i \cdot DI}{BW} \tag{1}$$

Fig. 2 Variations in pollutant concentrations in different sampling sites

where EC denotes pollutant concentration (mg/L); DI denotes daily ingestion, which is suggested by 2.0 L/day for adult, and 0.7 L/day for children; BW denotes body weight, which is assumed as 60 kg for adult, and 14.2 kg for children.

$$HQ_i = \frac{CDI_i}{RfD_i} \qquad (2)$$

where RfD denotes the oral toxicity reference dose values, which are determined as 0.0003, 0.0004, 0.04, 0.3, 0.0005, 0.0014, and 0.0015 mg/kg-day for As, Hg, Cu, Zn, Cd, Pb, and Cr, respectively. There are four scales of HQ: HQ≤1 (no risk), 1<HQ≤5 (low risk), 5<HQ≤10 (medium risk), and

HQ>10 (high risk).

Then, the carcinogenic risk (CR) can be calculated as follows (Ren et al. 2016; Dehghani et al. 2017):

$$\begin{cases} CR_i = CDI_i \cdot SF_i \\ CR = \sum CR_i \end{cases} \qquad (3)$$

where SF denotes the carcinogenic slope factors, which are suggested by 0.5, 15, and 1.5 mg/kg-day for Cd, Cr, and As, respectively. A CR value between 1×10^{-6} and 1×10^{-4} implies acceptable/tolerable carcinogenic risk; the risk changes to be unacceptable with a CR value higher than 1×10^{-4}, while it has no significant health hazards when the value is lower than 1×10^{-6}

Table 1 Statistical description of heavy metal and physicochemical parameters

| Items		S1	S2	S3	S4	S5	S6	S7	S8
pH	Min	7.25	7.31	7.17	7.38	7.18	7.26	7.31	7.23
	Max	8.51	8.60	8.01	7.96	8.63	7.61	7.82	7.74
	Mean	7.77	7.76	7.45	7.55	7.63	7.48	7.54	7.43
As (mg/L)	Min	0.00013	0.00016	0.00010	0.00030	0.00030	0.00040	0.00010	0.00060
	Max	0.00120	0.00080	0.00080	0.00110	0.00110	0.00170	0.00100	0.00180
	Mean	0.00063	0.00059	0.00057	0.00068	0.00073	0.00083	0.00064	0.00100
Hg (mg/L)	Min	0.00006	0.00005	0.00003	0.00004	0.00006	0.00004	0.00004	0.00009
	Max	0.00025	0.00025	0.00026	0.00026	0.00027	0.00030	0.00029	0.00034
	Mean	0.00013	0.00013	0.00014	0.00014	0.00014	0.00016	0.00014	0.00019
Cr (mg/L)	Min	0.00290	0.00292	0.00280	0.00280	0.00289	0.00289	0.00288	0.00281
	Max	0.00360	0.00380	0.00360	0.00360	0.00360	0.00365	0.00365	0.00500
	Mean	0.00336	0.00329	0.00324	0.00333	0.00327	0.00319	0.00331	0.00350
Cu (mg/L)	Min	0.04620	0.04360	0.04350	0.04660	0.04605	0.03620	0.04415	0.04320
	Max	0.05230	0.05250	0.05000	0.05120	0.05270	0.05420	0.05200	0.05300
	Mean	0.04898	0.04944	0.04867	0.04927	0.04928	0.04771	0.04849	0.04833
Pb (mg/L)	Min	0.00800	0.00850	0.00850	0.00860	0.00860	0.00838	0.00807	0.00776
	Max	0.01000	0.01000	0.01000	0.01000	0.01000	0.01015	0.01055	0.01095
	Mean	0.00971	0.00972	0.00934	0.00952	0.00929	0.00915	0.00937	0.00923
Zn (mg/L)	Min	0.01860	0.01950	0.01920	0.01970	0.02000	0.02000	0.01830	0.01800
	Max	0.06000	0.06000	0.07000	0.06000	0.08000	0.06000	0.06000	0.04200
	Mean	0.03738	0.03463	0.03577	0.03498	0.04292	0.03489	0.03328	0.02978
Cd (mg/L)	Min	0.00080	0.00086	0.00100	0.00080	0.00080	0.00070	0.00060	0.00050
	Max	0.00120	0.00130	0.00140	0.00140	0.00160	0.00180	0.00950	0.00100
	Mean	0.00110	0.00106	0.00107	0.00100	0.00095	0.00096	0.00159	0.00086

(Men et al. 2018).

Heavy metal pollution index

To evaluate the critical level of water quality, the heavy metal pollution index (HPI) is determined based on the weighted arithmetic mean calculation of selected parameters, which can be calculated as follows:

$$\begin{cases} W_i = \dfrac{k}{S_i} \\ Q_i = 100 \cdot \left(\dfrac{C_i}{S_i} \right) \\ HPI = \sum\limits_{i=1}^{n} \dfrac{Q_i \cdot W_i}{\sum\limits_{i=1}^{n} W_i} \end{cases} \quad (4)$$

where W_i denotes the weighting factors of each heavy metal; k
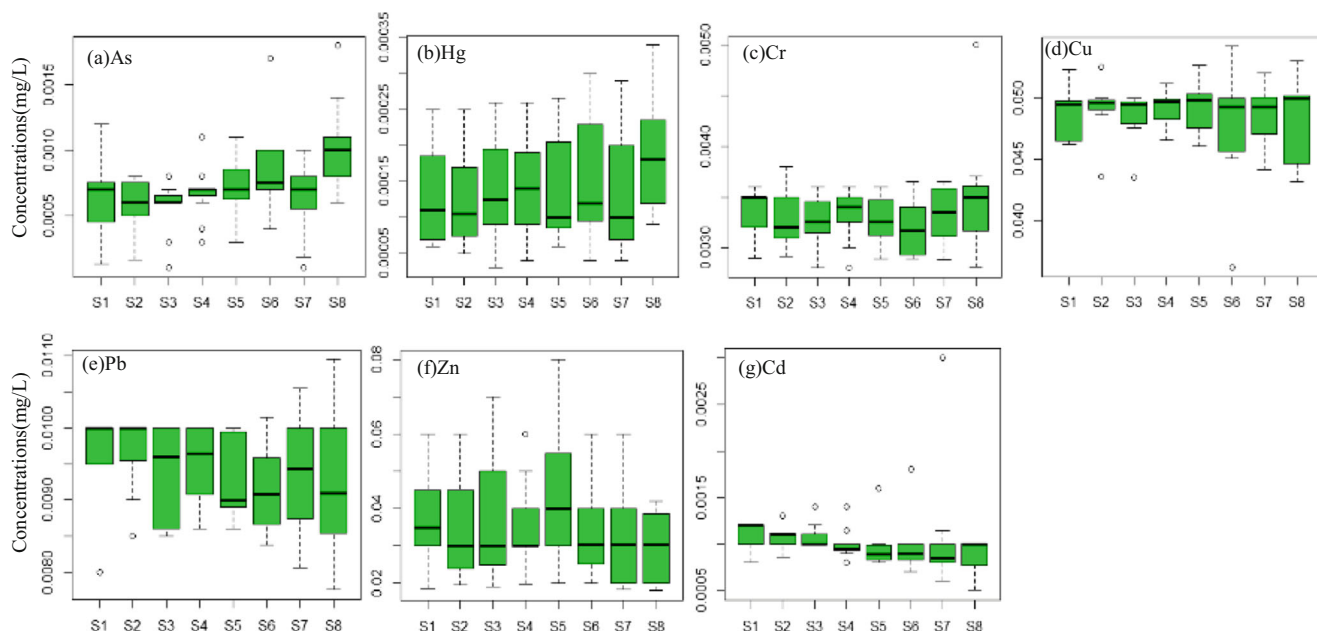
Fig. 3 Heavy metal variations in the aquatic environment of different sampling sites
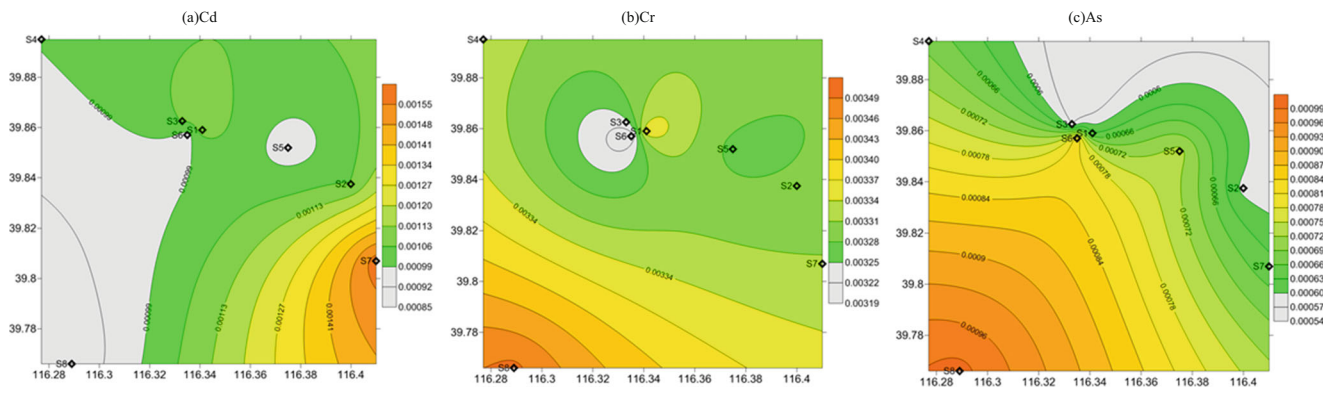
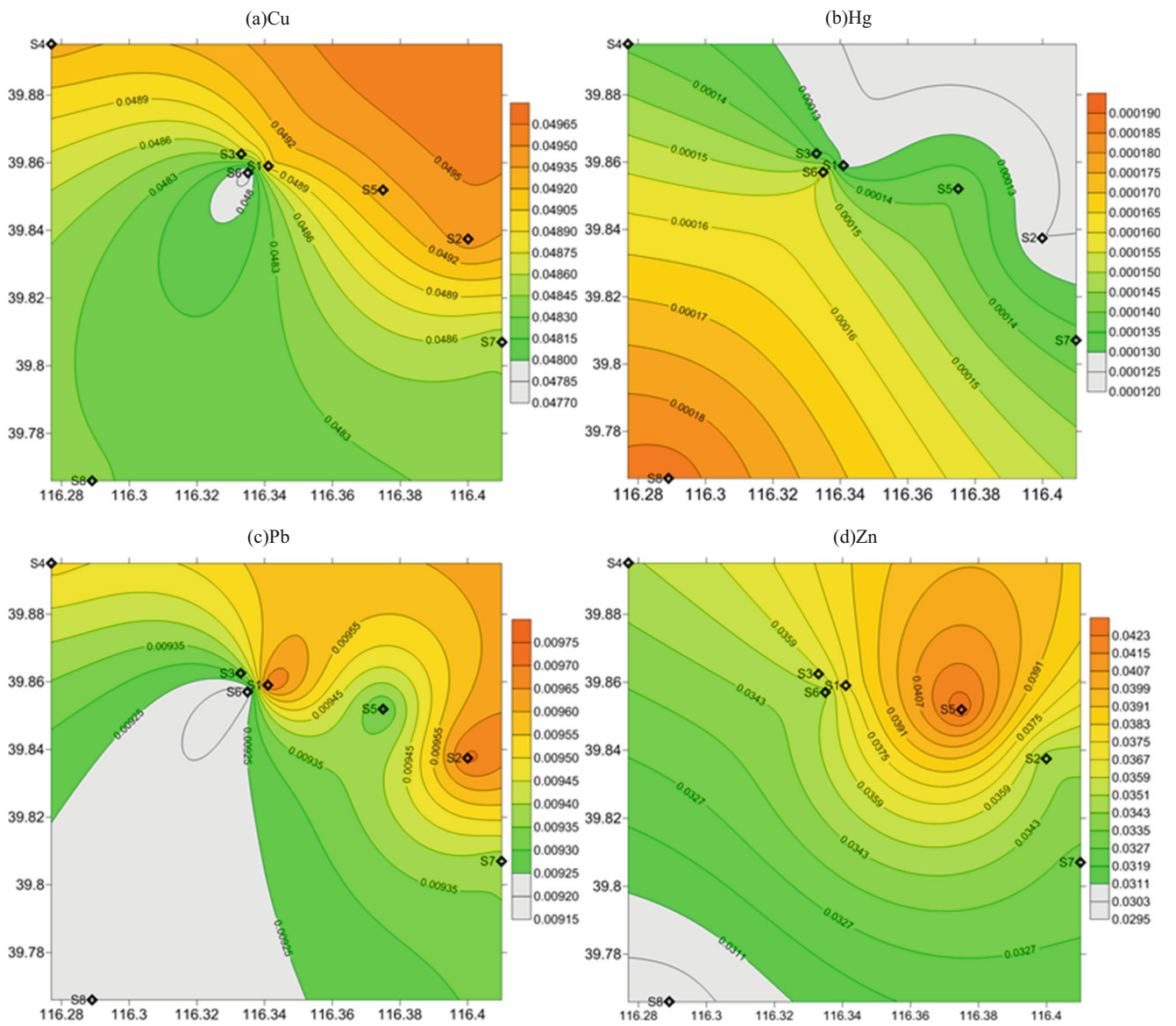**Fig. 4** Distribution patterns of carcinogenic HMs along the sample sites

Fig. 5 Distribution patterns of non-carcinogenic HMs along the sample sites

Table 2 Correlation matrix for heavy metals

	As	Hg	Cr	Cu	Zn	Pb	Cd
As	1.0000						
Hg	0.2190	1.0000					
Cr	0.4200	0.1500	1.0000				
Cu	− 0.0770	− 0.1690	0.0190	1.0000			
Zn	− 0.1360	− 0.1530	0.0360	0.0470	1.0000		
Pb	− 0.0510	− 0.3330	− 0.1190	0.2440	− 0.0760	1.0000	
Cd	− 0.2560	− 0.1540	− 0.1040	− 0.1250	− 0.1320	0.2590	1.0000

is the proportionality constant and is set as 1 in this study; S_i denotes the desirable limit of each heavy metal given by regulatory standard; C_i denotes the average concentration of each heavy metal; Q_i denotes the sub-index of each heavy metal. When HPI ≤ 100, it means that the contamination of HMs in the aquatic environment could be acceptable.

Monte Carlo–based uncertainty analysis

Uncertainties associated with carcinogenetic risk could be conducted into a matrix and vectors based on Monte Carlo simulation, during which each execution generates a sample output. The output can then be stochastically analyzed for identifying the corresponding cumulative probability distributions. Generally, the detailed Monte Carlo process can be summarized as follows: (a) producing lots of random numbers for each stochastic input; (b) according to a special statistical distribution, these random numbers could be transformed into the related random variates; (c) storing the obtained stochastic variates in an array for each parameter; (d) each parameter would generate a value, which is used as a deterministic input in the computation formula of the allowable carcinogenetic risk; (e) computing the acceptable carcinogenetic risk based on a numerical model for each Monte Carlo run; (f) the outputs of the acceptable carcinogenetic risk would be stored; (g) repeating Steps (a)–(f) for specified Monte Carlo runs; and (h) analyzing the calculation results and achieving a cumulative probability distribution. Carcinogenic risk describes the probability when human beings are exposed to cancer-causing contaminants like heavy metals. It is one of the most concerning health problems in human beings. Therefore, it is significant to accurately evaluate the level of carcinogenic risk. However, quantitative calculation of carcinogenic risk involves parameters with a mount of uncertainties. The value of these parameters (e.g. slope factors and daily ingestion) are recommended by USEPA, based on numerous animal toxicity experiments. It is hard to accurately predict the value for humans in this special case (a case study

of China). The uncertainty of parameters can directly influence the accuracy of carcinogenic health risk assessments. Monte Carlo simulation is one of the most effective methods to solve the randomness and uncertainty within model operations. Moreover, sensitivity analysis could be given to determine the impacts of modeling components or modeling inputs on the final results of carcinogenetic risk. Sensitivity analysis could reflect the impacts of parameters uncertainties on carcinogenic risk calculation and make the values of carcinogenic risk of heavy metals close to the "real" ones.

Results and discussion

Compositional analysis and identification of pollution sources

The statistical descriptions of HMs and the physicochemical parameters with minimum, maximum, and mean values are presented in Table 1. The HM variations in the aquatic environment are illustrated in Fig. 3. The monitoring data of all the seven heavy metals were measured by the official government considering Environmental Quality Standards for Surface Water of National Standard of China (GB3838-2002). In this

Table 3 Loading scores of heavy metals to each component

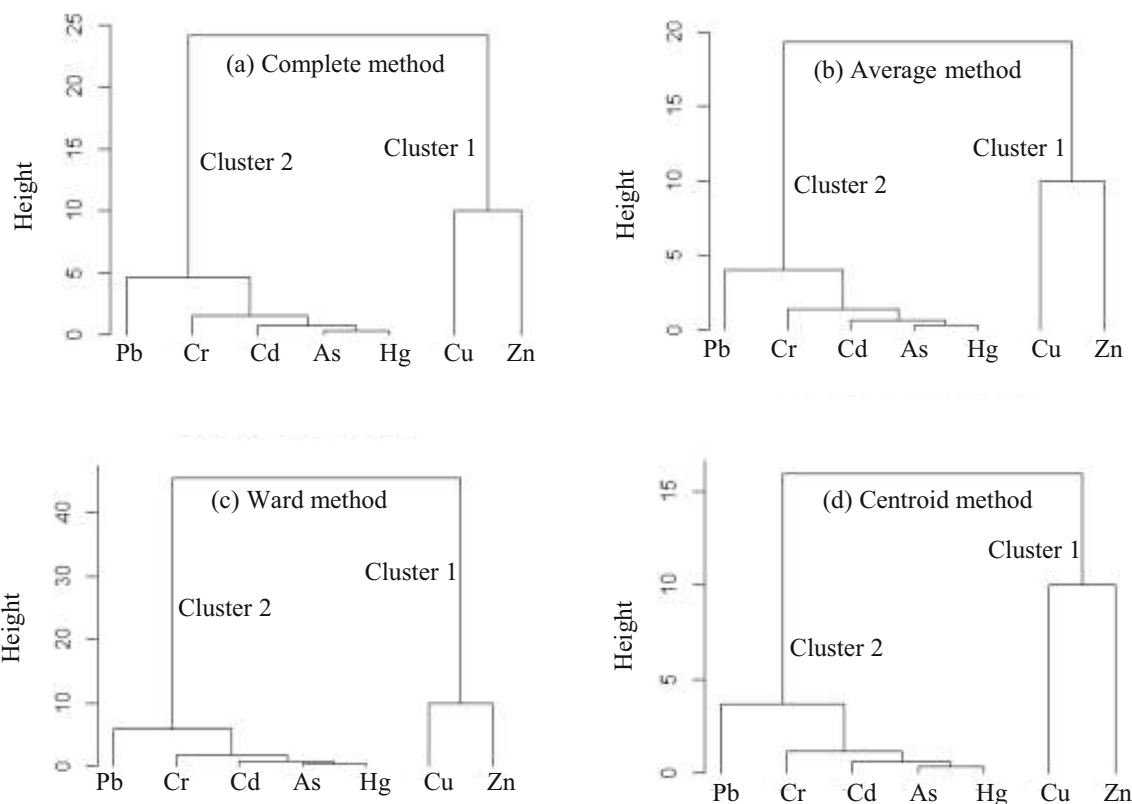|	Comp. 1	Comp. 2	Comp. 3	Comp. 4
As	− 0.457	0	− 0.386	− 0.256
Hg	− 0.446	0.226	0.187	0.583
Cr	− 0.427	0	− 0.223	− 0.525
Cu	0.256	− 0.467	− 0.508	0.408
Zn	0.455	0.127	− 0.397	− 0.192
Pb	0	− 0.632	0.551	− 0.266
Cd	0.362	0.552	0.218	− 0.214
Eigenvalue	1.7575	1.1909	1.0731	0.8590
Proportion of variance (%)	44.126	20.263	16.449	10.543
Cumulative proportion (%)	44.126	64.389	80.838	91.381

Fig. 6 Clustering tree of the HMs based on different methods

work, the pH values varied between 7.17 and 8.63, and the mean value is 7.58 for the aquatic environment. All water samples showed neutral to slightly alkaline pH level, and no contamination by acidic pollutants was noted. S8 had high concentrations of As, Hg, and Cr; S4 had high concentrations of Cu; S1 and S2 had high values of Pb; and S5 and S7 had high concentrations of Zn and Cd, respectively. According to the mean concentrations in the water samples, the metals followed this decreasing order of concentration: Cu > Zn > Pb > Cr > Cd > As > Hg. All of them met the water quality standard of GB3838–2002 grade III. The mean concentration of HMs and their spatial distribution patterns along the sample sites are displayed in Figs. 4 and 5, respectively. As can be seen in Fig. 4, the concentration of Cd in the studied samples was less than 0.0095 mg/
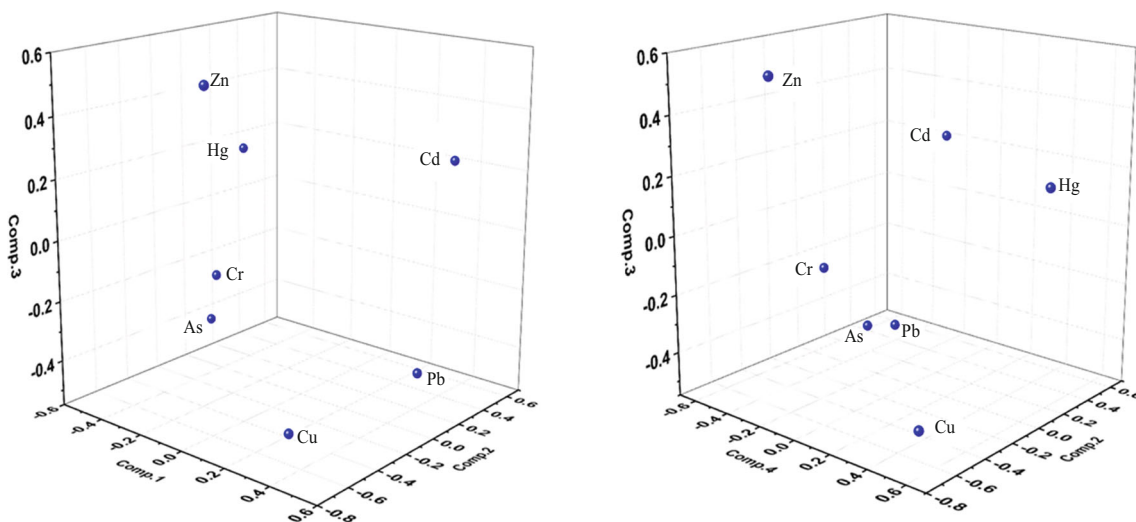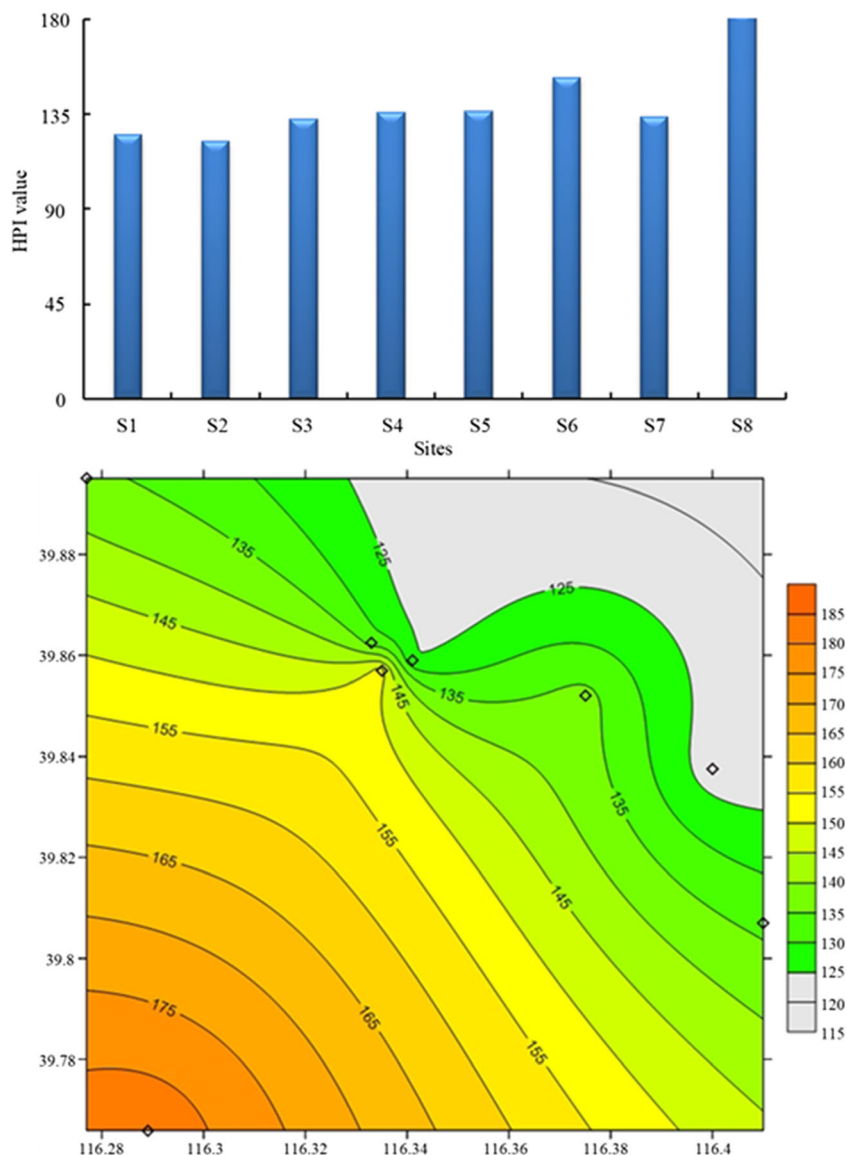

Fig. 7 Principal component analysis of HMs concentrations in aquatic environment

Fig. 8 Solutions of HPI along the sampling sites

L, with the mean value being 0.0011 mg/L. The common sources of Cd in the aquatic environment are the

burning of fossil fuels, wastewater from industrial and urban effluence, and agriculture activities. The Cr level mainly ranged from 0.0028 to 0.0050 mg/L, with a mean of 0.0033 mg/L; hence, it did not exceed the permissible limit of grade III water quality of 0.0050 mg/L. In terms of As concentration, it ranged from 0.0001 to 0.0018 mg/L, with a mean of 0.0007 mg/L. Located downstream of the river, S7 and S8 showed relatively high values of Cd, Cr, and As. As illustrated in Fig. 5, the concentration of Cu was within the permissible limit of l.0 mg/L. A high Cu concentration was observed at S2 and S4, possibly because of the presence of copper bucket industries in these two areas. Meanwhile, Zn is an important micronutrient for ensuring proper metabolic processes in living organisms. However, high Zn levels could exert a negative impact
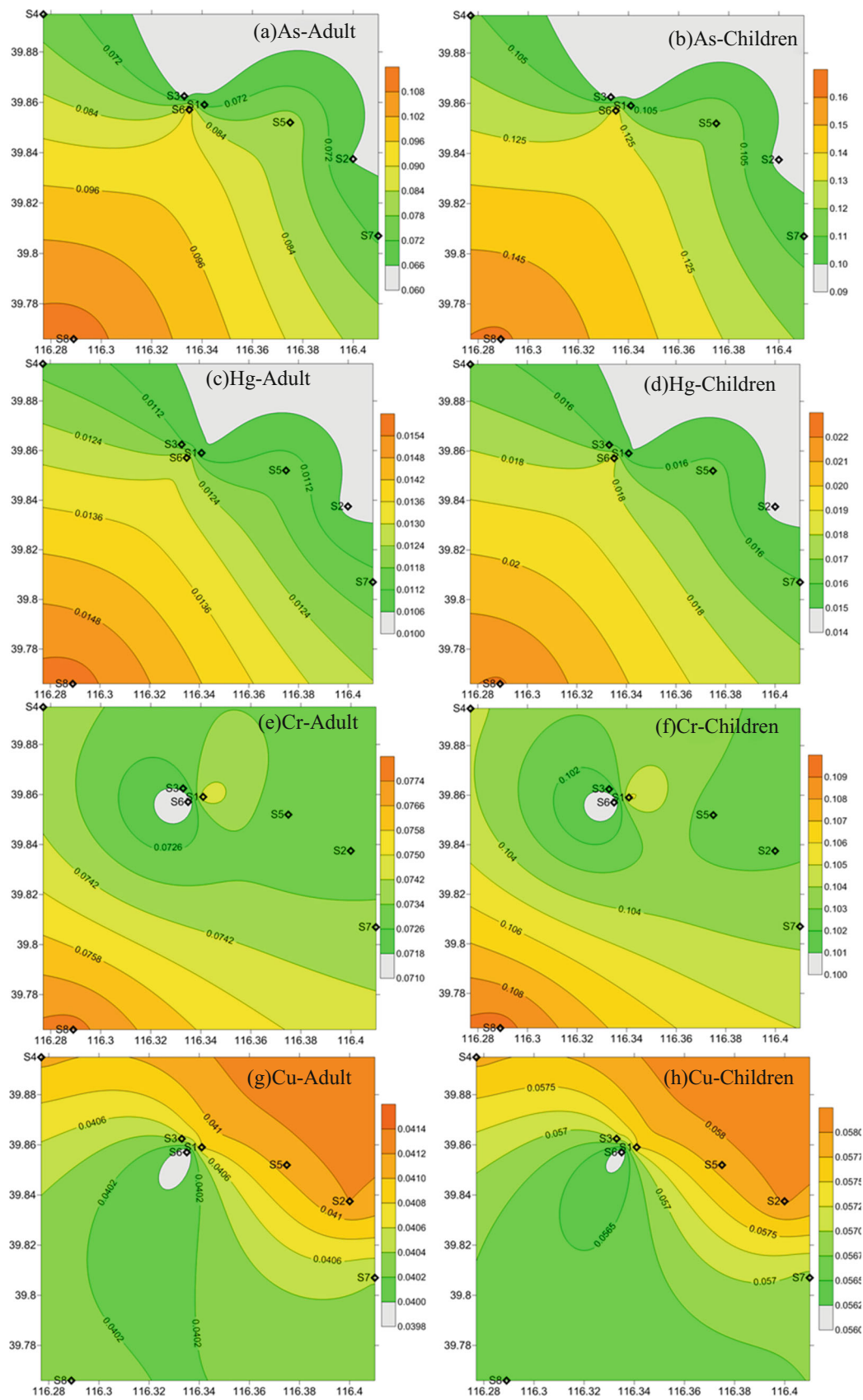
Table 4 Description of the mean CDI and HQ for adult and children through ingestion

HMs	CDI (adult)	CDI (children)	HQ (adult)	HQ (children)
As	2.36E−05	3.33E−05	0.079	0.111
Hg	4.79E−06	6.74E−06	0.012	0.017
Cu	1.63E−03	2.29E−03	0.041	0.057
Zn	1.18E−03	1.66E−03	0.004	0.006
Cd	3.58E−05	5.04E−05	0.072	0.101
Pb	3.14E−04	4.42E−04	0.224	0.316
Cr	1.10E−04	1.55E−04	0.074	0.104

Fig. 9 Distribution of hazard quotient (HQ) indices of HMs in the aquatic environment
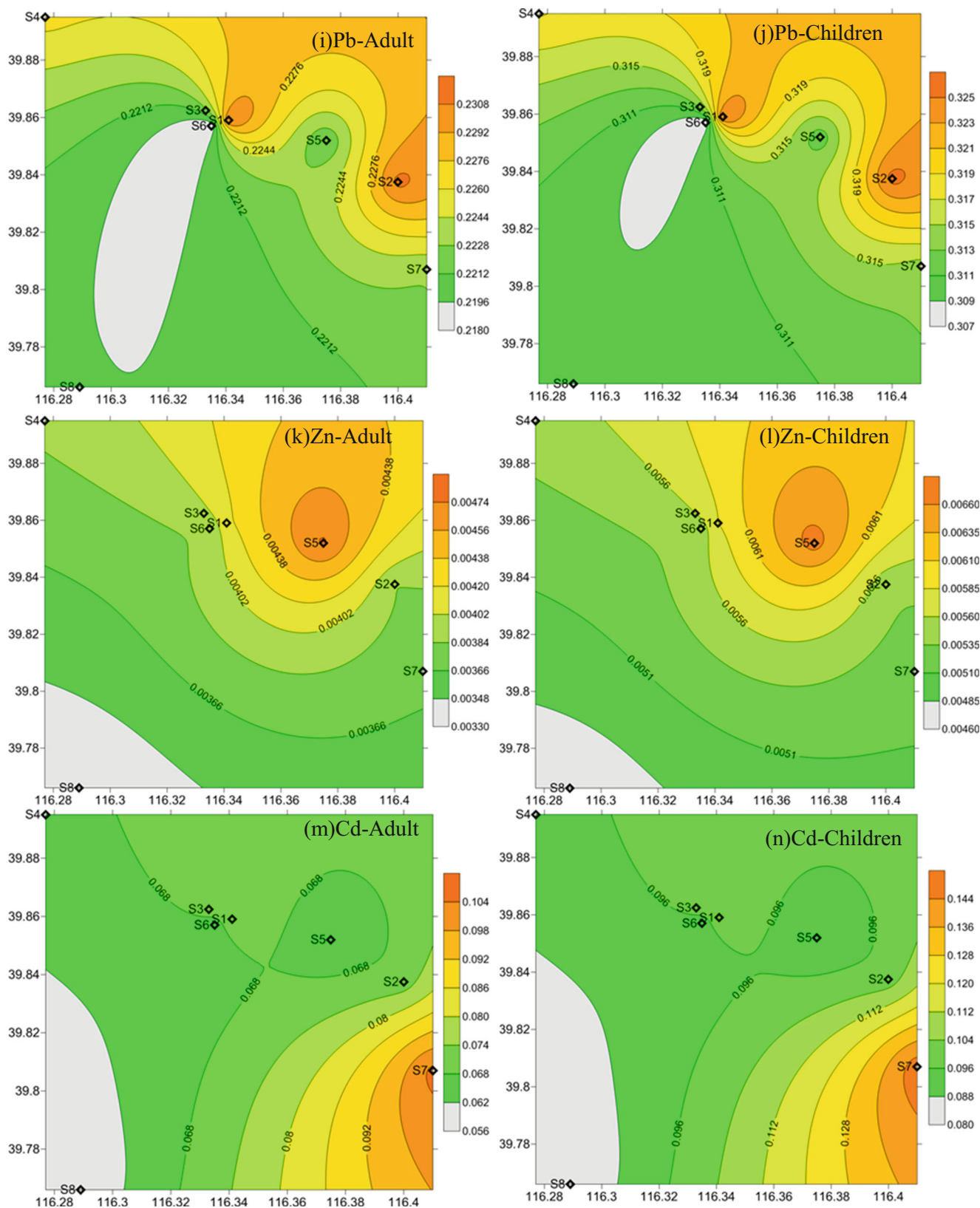
Fig. 9 (continued)

Table 5 Carcinogenic risks As, Cd, and Cr for adult and children through ingestion	Sites	As (adult)	Cd (adult)	Cr (adult)	As (children)	Cd (children)	Cr (children)
	S1	1.400E−05	7.306E−05	7.472E−06	1.972E−05	1.029E−04	1.052E−05
	S2	1.311E−05	7.089E−05	7.300E−06	1.847E−05	9.984E−05	1.028E−05
	S3	1.267E−05	7.111E−05	7.204E−06	1.784E−05	1.002E−04	1.015E−05
	S4	1.511E−05	6.633E−05	7.407E−06	2.128E−05	9.343E−05	1.043E−05
	S5	1.622E−05	6.356E−05	7.267E−06	2.285E−05	8.951E−05	1.023E−05
	S6	1.844E−05	6.417E−05	7.094E−06	2.598E−05	9.038E−05	9.992E−06
	S7	1.422E−05	1.058E−04	7.363E−06	2.003E−05	1.490E−04	1.037E−05
	S8	2.222E−05	5.755E−05	7.772E−06	3.130E−05	8.106E−05	1.095E−05

on such processes, especially from a long-term perspective. In the study area, the average concentration of Zn was 0.284 mg/L, which was within the safe limit. S5 showed higher Zn levels than the other sites. As for Pb contamination, its concentration ranged from 0.007 to 0.011 mg/L, with a mean of 0.0094 mg/L. The major source of Pb contamination was identified to be anthropogenic activities. For example, the extensive application of fossil fuels in thermal power plants might lead to high Pb contaminations in S1 and S2. The concentrations of heavy metals are directly influenced by the nearby industrial activities.

Table 2 presents the correlation matrix for heavy metals. Pearson's correlation analysis indicated that the correlations between different HMs were weak and not significant ($p > 0.05$), except for As and Cr. The poor correlations might be due to the geochemical behaviors of the parameters and the differences in the sources of HMs, implying that non-point sources exhibited strong contamination characteristics, such as contamination distributing disperses, component complexities, and contamination approach diversity. Additionally, CA was conducted to classify the HMs in the surface water dataset. Multiple tools, including the complete method, average method, ward method, and centroid method, were applied to visualize this process. The corresponding results are displayed in Fig. 6. The results showed that regardless of the model used, the two major clusters were (1) Pb Cr Cd As Hg and (2) Cu Zn. Moreover, PCA was used to conduct composition analysis, as it could help reduce the dimension of multivariate data and provide useful information associated with the significant parameters present in the whole dataset. Hence, its application greatly reduces the complexities of the evaluation framework. Four principal components explained 91.381% of the total variance (Table 3 and Fig. 7), with 44.126%, 20.263%, 16.449%, and 10.543% of the variance explained by Comp. 1, Comp. 2, Comp. 3, and Comp. 4, respectively. Comp. 1 loaded strongly on As, Hg, Cr, and Zn, and these metals were mostly from natural sources and industry activities. Comp. 2 was mainly composed of Cu, Pb, and Cd possibly because of the extensive utilization of fossil fuels and wastewater emissions. Comp. 3 exhibited high loadings of Cu because of the copper bucket industries around this river. Comp. 4 showed high loadings of Hg and Cr, from natural sources. The above results indicate the sources of the seven heavy metals and their interrelations.
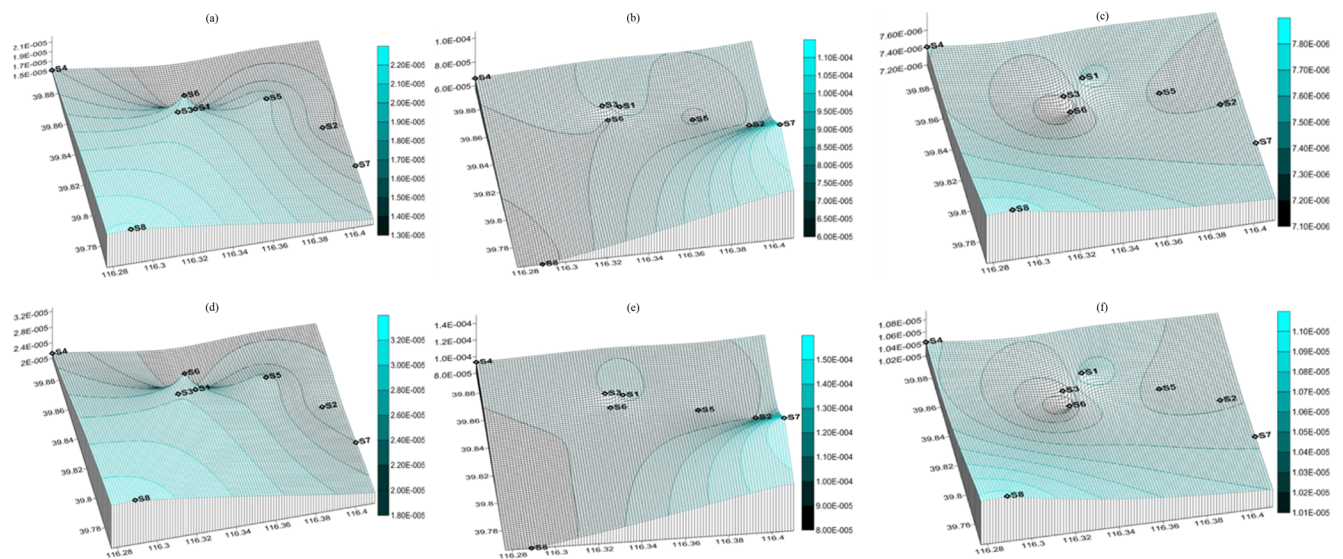
Fig. 10 Distribution of carcinogenic risk (CR) indices of As, Cd, and Cr in the aquatic environment

Fig. 11 Variations in hazard quotient and carcinogenic risk along the sampling sites
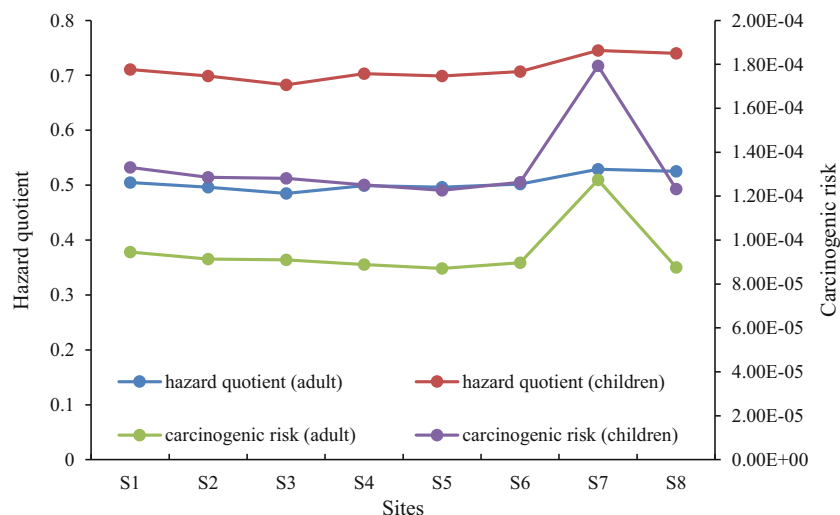
HPI analysis

PIs, such as the HPI, were evaluated for different sampling sites in the aquatic environment. The results are displayed in Fig. 8. All of these HPI values were significantly higher than the critical level (i.e., 100), thus implying that this aquatic environment was contaminated by multiple HMs. High HPI values were observed in S5, S6, and S8 while low HPI values were noted in S1 and S2. Hence, the upper and middle parts of this river had high contaminations while the downstream of this river had slight loadings. This result might be attributed to a large number of production and living activities upstream and dilution and flushing effect by the natural discharge of the river.

Potential risk assessment for human health

HMs are potentially harmful to human health, and HQ could be used to assess the risks of chronic health through the ingestion of water. CDI represents the daily exposure of the population to HM contaminations in mg/kg-day. The descriptions of the mean CDI and HQ for adults and children through ingestion are presented in Table 4. The CDI values in both groups showed that water was Cu > Zn > Pb > Cr > Cd > As>

Hg type, with Cu in the highest CDI value (1.63E–0.3 for adults and 2.29E−0.3 for children) among all metals. Figure 9 illustrates the distribution of HQ values of HMs with consideration of the two receptors (i.e., adults and children). The HQ values of all sampling sites were below 1 and ranged from 0.48 to 0.74, which indicated a low non-carcinogenic hazard. The results showed that the sampling sites in this study area followed the decreasing order of HQ values: S7 > S8 > S1 > S6 > S4 > S2 > S5 > S3. Such a tendency revealed that the HQ value in the northern section of the aquatic environment was significantly higher than that in the southern and central sections. Additionally, HMs followed the decreasing order of HQ values: Pb >As > Cr > Cd > Cu > Hg >Zn. The total HQ value for children reached 5.69, which was 1.65 times higher than that for the adults. In terms of different HMs, Pb (0.224 mg/kg-day for adult and 0.316 mg/kg-day for children) had the greatest health risk with a total HQ value of 2.53, especially in S1, followed by As (0.079 mg/kg-day for adults and 0.111 mg/kg-day for children) with a total HQ value of 0.89, especially in S8. Thus, these two pollutants should be controlled for the purpose of public safety.

Among these HMs, As, Cd, and Cr pose significant carcinogenic risks to the public. As shown in Fig. 10 and Table 5, the carcinogenic risk of Cd was the highest, especially in S1, S3, and S7, with some values exceeding 1×10^{-4} for adults and children. These values indicated unacceptable carcinogenic risks. The CR values of other metals (i.e., As and Cr) for all populations were between 1×10^{-6} and 1×10^{-4}, implying acceptable or tolerable carcinogenic risks. Although the insignificant carcinogenic risks posed to the public are insignificant, decision-makers should pay attention particularly to children because most values exceeded 1×10^{-5}. Additionally, the sampling sites followed the decreasing order of CR values: S7 > S1 > S2 > S3 > S6 > S4 > S8 >S5. This result is due to S7 comprising many industries, which generate wastewater that could increase HM concentrations. For example, Cd emitted from industrial activities might enter the

Table 6 Parameters of the model for probabilistic risk assessment

Parameters	Unit	Mean	Minimum	Maximum
DI (adult)	L/day	2.0	1.5	3.2
DI (children)	L/day	0.6	0.5	1.5
BW (adult)	kg	61.0	60.0	64.3
BW (children)	kg	18.2	14.2	22.9
SF-Cd	mg/(kg-day)	1.3	0.5	6.1
SF-Cr	mg/(kg-day)	23.0	15.0	41.0
SF-As	mg/(kg-day)	2.2	1.5	15.0

Table 7 Quantile statistics of carcinogenic risks for adult and children

| Quantile	Cd (adult)	Cd (children)	As (adult)	As (children)	Cr (adult)	Cr (children)	Total (adult)	Total (children)
10%	1.90E−04	2.50E−04	6.00E−05	7.00E−05	1.20E−05	4.20E−05	2.90E−04	3.80E−04
20%	2.20E−04	2.90E−04	6.00E−05	9.00E−05	1.30E−05	4.60E−05	3.30E−04	4.40E−04
30%	2.40E−04	3.30E−04	7.00E−05	1.00E−04	1.40E−05	5.00E−05	3.60E−04	4.90E−04
40%	2.70E−04	3.70E−04	8.00E−05	1.00E−04	1.40E−05	5.30E−05	3.90E−04	5.40E−04
50%	3.00E−04	4.10E−04	8.00E−05	1.10E−04	1.50E−05	5.70E−05	4.20E−04	5.90E−04
60%	3.30E−04	4.60E−04	9.00E−05	1.20E−04	1.60E−05	6.00E−05	4.50E−04	6.50E−04
70%	3.60E−04	5.20E−04	9.00E−05	1.40E−04	1.70E−05	6.40E−05	4.90E−04	7.10E−04
80%	4.10E−04	6.00E−04	1.00E−04	1.50E−04	1.90E−05	6.90E−05	5.40E−04	7.90E−04
90%	4.90E−04	7.30E−04	1.10E−04	1.70E−04	2.00E−05	7.60E−05	6.20E−04	9.30E−04

aquatic environment through atmospheric sedimentation and surface runoff, eventually enriching the sedimentation environment. Generally, variations in hazard quotient and carcinogenic risk along the sampling sites are illustrated in Fig. 11.

Uncertainty analysis

Uncertainty, especially as stochastic property, extensively exist in the water quality evaluation framework. In this study, the Monte Carlo simulation method as a widely used tool is applied for better understanding the variations in carcinogenic risk, during which the majority of parameters were assumed as triangular distributions (Table 6). For example, the concentrations of As, Cd, and Cr are presented as a triangular

distribution with determining their maximum, minimum, and mean values as shown in Table 1.

Figures 12, 13 and 14 show the probability distributions of the carcinogenic risks of As, Cd, and Cr for adults and children. With regard to these two populations, the CR values followed the order Cd > As > Cr. The Monte Carlo results revealed that regardless of the quantile considered, the CR value of Cd was significantly higher than 1×10^{-4}, even reaching 7.3×10^{-4} for children under the 90th quantile (Table 7). In terms of As, its mean carcinogenic risks were 0.8×10^{-4} and 1.2×10^{-4} for adults and children, respectively. Their resulting 90th quantile values respectively reached 1.1×10^{-4} and 1.7×10^{-4} (Table 7), thus exceeding 1×10^{-4} and indicating obvious carcinogenic risks for both populations. Relative to those of Cd and As, all CR values of Cr
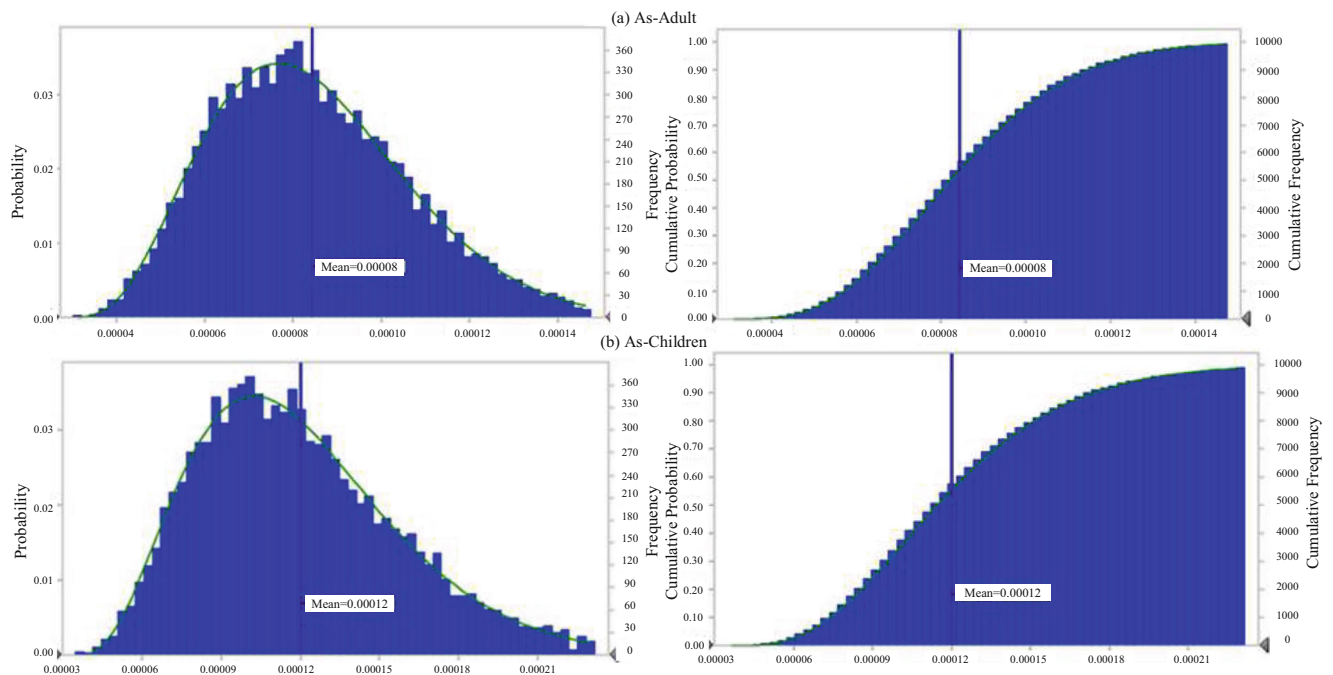
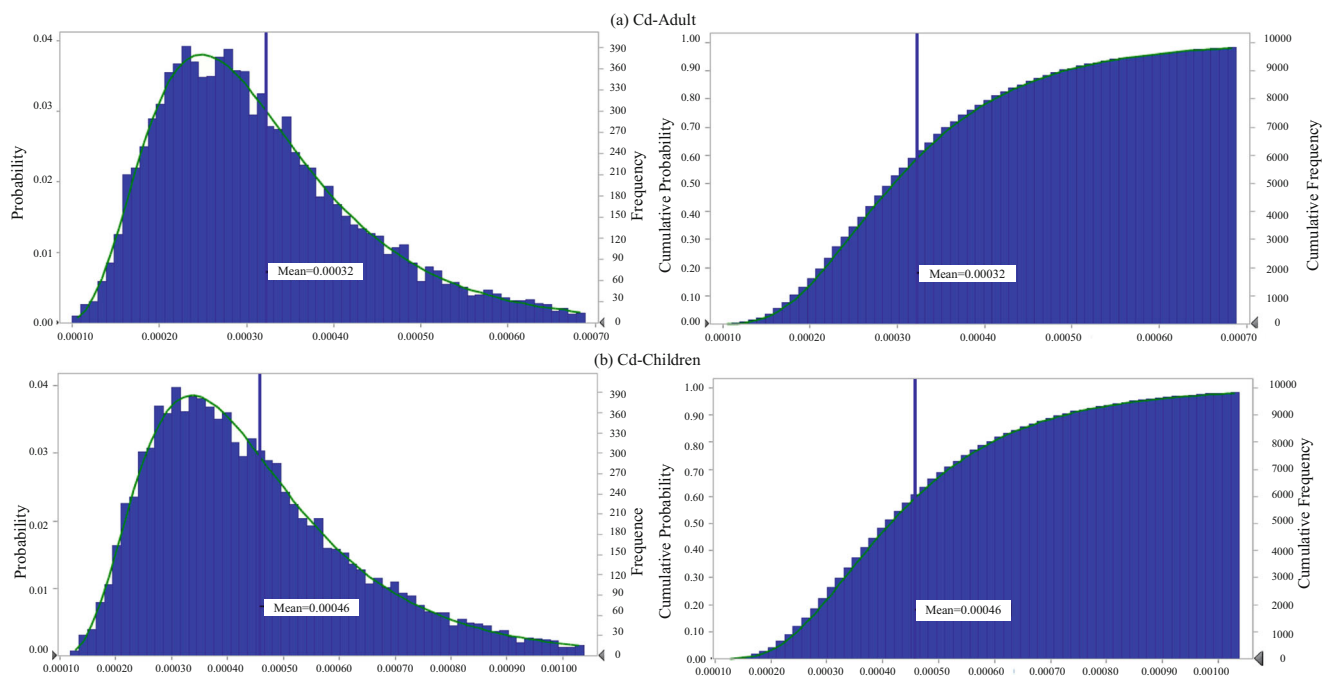**Fig. 12** Probability distributions of As carcinogenic risk for adult and children

Fig. 13 Probability distributions of Cd carcinogenic risk for adult and children

were below the risk threshold, with the mean carcinogenic risks being 0.16×10^{-4} and 0.58×10^{-4} for adults and children, respectively. In addition, the total carcinogenic risks respectively reached 4.4×10^{-4} and 6.3×10^{-4} for adults and children on average (Fig. 15). Their corresponding 90th quantile values changed to 6.2×10^{-4} and 9.3×10^{-4}. Cd contributed over 70% to the total carcinogenic risk, followed by As (above 19%). Moreover, sensitivity analysis indicated that

daily ingestion and slope factors exerted significant impacts on the total carcinogenic risk as they accounted for 40.8% and −35.5% of the total, respectively (Fig. 16). The results also indicated that the concentration of Cd in S7 had a moderate impact (i.e., 13.1%) on the total carcinogenic risk; the other was mostly contributed by body weight (i.e., −7.9%). In general, uncertainties relative to modeling parameters exerted significant effects on the final CR solutions. A high quantile
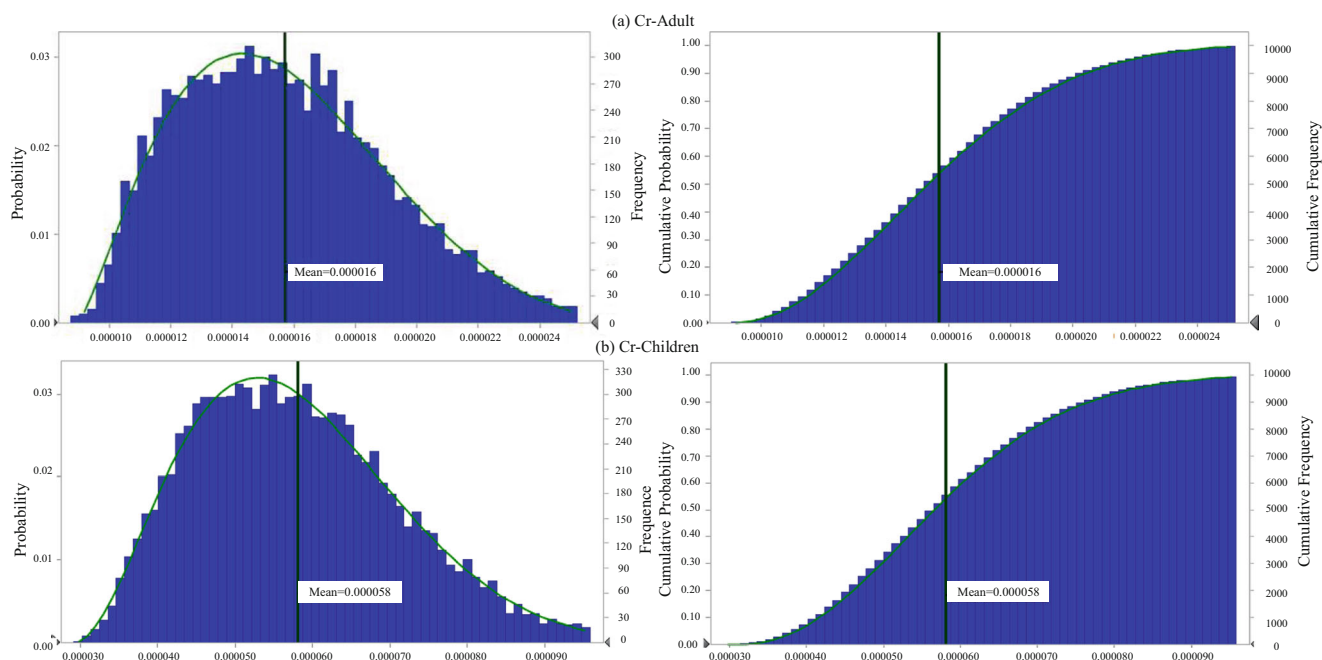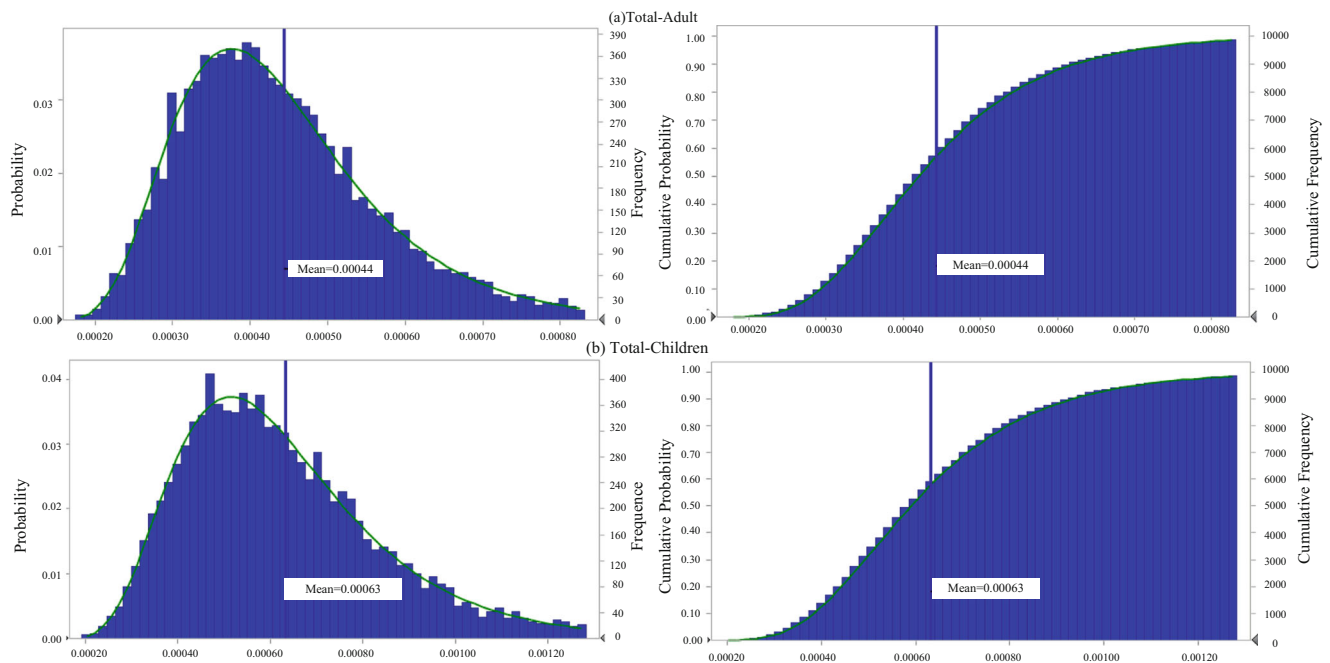

Fig. 14 Probability distributions of Cr carcinogenic risk for adult and children

**Fig. 15** Probability distributions of the total carcinogenic risk for adult and children

corresponded to a high CR value and a low standard-reaching rate; conversely, a low quantile led to a low CR value and then to a high probability of acceptable risks. These results could help decision-makers coordinate the conflict interaction between carcinogenic risks and system reliability.

Actually, each step of health risk assessment is full of uncertainty. In this study, majority of parameters for carcinogenic risk are taken into consideration. Surely, the overall effects of other coefficients and risk assessment kinds may hardly be ignored. Moreover, the steps and evaluation criterion of health risk assessment are recommended by the U.S. EPA. Although parameter values are scientifically based on statistics of a large amount of toxicological experiments, they are not absolutely suitable for all case studies from different countries. It is thus desired that a new system for health risk assessment of our own country should be developed as soon as possible, which is applicable to local conditions.

Conclusions and recommendations

This study proposes an evaluation framework for characterizing and quantifying the sources and contamination degrees of heavy metal contamination in the North Canal of Fengtai District, China. The framework could exhibit the impacts of heavy metals on human health and their relationships with uncertainties by integrating multidisciplinary approaches, involving multivariate statistical method, health risk assessment, and uncertainty analysis. Results indicated that (1) the downstream of the river had higher concentrations of Cd, Cr, and As; sources of Cd were identified as domestic and industrial wastewater, consumption of fossil fuels, as well as agriculture activities; (2) Pearson's correlation analysis revealed that the correlations between different HMs were weak and not significant ($p > 0.05$), except for As and Cr, which was mostly owing to geochemical behaviors of parameters and

Fig. 16 Sensitivity analysis of the total carcinogenic risk
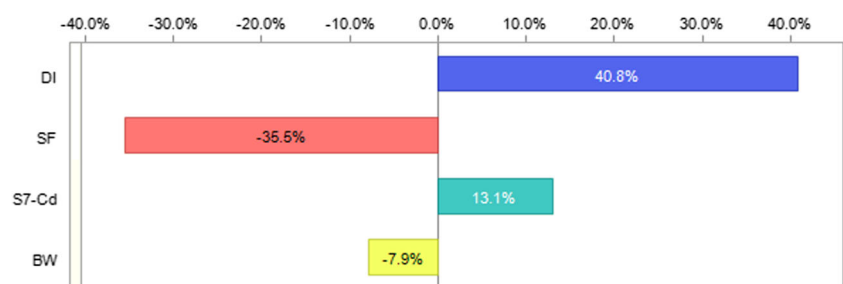
differences in sources of heavy metals. There were two major clusters: Pb Cr Cd As Hg and Cu Zn; (3) principal component analysis showed that four principal components were given to explain 91.381% of the total variance. Solutions from HPI values presented that they were significantly higher than the critical level, especially in S5, S6, and S8, implying that this aquatic environment has been contaminated by multiple HMs; (4) health risk assessment demonstrated that all HQ values in each sampling sites ranged from 0.48 to 0.74, representing a low non-carcinogenic hazard; and HQ value in the northern section of the aquatic environment was significantly greater than that in the southern and central sections. The highest carcinogenic risk was from Cd in S1, S3, and S7 with unacceptable carcinogenic risks. The CR values of As and Cr were lower than acceptable carcinogenic risks; (5) uncertainty analysis disclosed that a low quantile led to a low CR value, and then to a high probability of the acceptable risk. Conversely, a higher quantile corresponded to a higher CR value and a lower standard-reaching rate. These results could help decision-makers coordinate the conflict interaction between carcinogenic risk and system reliability. Sensitivity analysis indicated that both daily ingestion and slope factors had significant impacts on the total carcinogenic risk, accounting for 40.8% and − 35.5%, respectively.

As multiple complicated characteristics were merged into the evaluation framework, difficulties emerged with regard to addressing the evaluation issues exclusively on the basis of mathematical approaches, particularly when uncertainties were considered in the decision-making process. Although all the concentrations of HMs met the standard of GB3838-2002 grade III, their carcinogenic risks and other pollutants should attract the attention of decision-makers. Some effective management measures should also be taken to ensure water safety. For example, regulation of pollutant sources (Wang et al. 2015), and development of advanced technologies for treating wastewater in municipal wastewater treatment plants. Any human activities within the areas with higher environmental risks (i.e., S7 and S8) should be also prohibited to the most extent.

The specific recommendations of this work could be summarized as follows. Firstly, thorough investigations are obviously needed. With respect to the upstream performances being significantly better than the downstream performance, the junction of S1, S5, and S2 should be studied with a focus on the key pollutant discharging enterprises along the river. The objective is to identify explicitly the channels and patterns of pollutant discharge, which could lay the foundation for the diversion of rain and wastewater. Secondly, remediation requires unification. Local governments should construct infrastructure and protection facilities to protect water resources. To ensure water quality and water supply to the river, they should conduct sewage interception that will prevent secondary pollution. Thirdly, supervision should also be

strengthened through the enforcement of environmental laws and regulations, particularly those pertaining to illegal activities. It is also required to strengthen identification of risk sources, assessment of environmental risks, and disposal of emergency. Finally, publicity and education for local people should be improved by emphasizing the significance of the health and biodiversity of the ecosystem (Zhang et al. 2017).

Two concerns should be addressed in future studies. On the one hand, this study only assesses seven heavy metals, probably leading to an unrealistic state of heavy metal contamination in the aquatic environment. Therefore, more heavy metal types should be integrated into the improved evaluation framework to comprehensively reflect the real status of heavy metal contamination. On the other hand, in most cases, there might be more uncertain information (e.g., interval and fuzzy parameters) associated with the modeling inputs. Future studies will be required to deal with the impacts of multiple uncertainties on the health risks of heavy metals.

Data availability The datasets used and/or analyzed during the current study are available from the corresponding author on reasonable request.

Compliance with ethical standards

Ethics approval and consent to participate   Not applicable.

Consent to publish   Not applicable.

Competing interests   The authors declare that they have no competing interests.

References

Albuquerque MTD, Gerassis S, Sierra C, Taboada J, Martin JE, Antunes IMHR, Gallego JR (2017) Developing a new Bayesian risk index for risk evaluation of soil contamination. Sci Total Environ 603: 167–177. https://doi.org/10.1016/j.scitotenv.2017.06.068

Astel A, Tsakovski S, Barbieri P, Simeonov V (2007) Comparison of self-organizing maps classification approach with cluster and principal components analysis for large environmental data sets. Water Res 41(19):4566–4578. https://doi.org/10.1016/j.watres.2007.06.030

Bartoli G, Papa S, Sagnella E, Fioretto A (2012) Heavy metal content in sediments along the Calore river: relationships with physical-chemical characteristics. J Environ Manag 95:S9–S14. https://doi.org/10.1016/j.jenvman.2011.02.013

Bayo J, López-Castellanos J (2016) Principal factor and hierarchical cluster analyses for the performance assessment of an urban wastewater treatment plant in the southeast of Spain. Chemosphere 155:152–162. https://doi.org/10.1016/j.chemosphere.2016.04.038

Chen YZ, Lu HW, Li J, Huang GH, He L (2016) Regional planning of new-energy systems within multi-period and multi-option contexts: a case study of Fengtai, Beijing, China. Renew Sust Energ Rev 65:356–372. https://doi.org/10.1016/j.rser.2016.07.017

Chen YZ, Lu HW, Li J, Ren LX, He L (2017) A leader-follower-interactive method for regional water resources management with considering multiple water demands and eco-environmental constraints. J Hydrol 548:121–134. https://doi.org/10.1016/j.jhydrol.2017.02.015

De Silva S, Ball AS, Huynh T, Reichman SM (2015) Metal accumulation in roadside soil in Melbourne, Australia: effect of road age, traffic density and vehicular speed. Environ Pollut 208:102–109. https://doi.org/10.1016/j.envpol.2015.09.032

Deepa J, Jitendra P (2019) Investigations on peculiarities of land-water interface and its use as a stable testbed for accurately predicting changes in ecosystem responses to human perturbations: a sub-watershed scale study with the Ganga River. J Environ Manag 238:178–193. https://doi.org/10.1016/j.jenvman.2019.02.126

Dehghani S, Moore F, Keshavarzi B, Hale BA (2017) Health risk implications of potentially toxic metals in street dust and surface soil of Tehran, Iran. Ecotox Environ Safe 136:92–103. https://doi.org/10.1016/j.ecoenv.2016.10.037

Delpal I, Florea M, Pelletier G, Rodriguez MJ (2018) Optimizing disinfection by-product monitoring points in a distribution system using cluster analysis. Chemosphere 208:512–521. https://doi.org/10.1016/j.chemosphere.2018.06.009

Devi NL, Yadav IC (2018) Chemometric evaluation of heavy metal pollutions in Patna region of the Ganges alluvial plain, India: implication for source apportionment and health risk assessment. Environ Geochem Hlth 40(6):2343–2358. https://doi.org/10.1007/s10653-018-0101-4

Eze PN, Madani N, Adoko AC (2019) Multivariate mapping of heavy metals spatial contamination in a Cu-Ni exploration field (Botswana) using turning bands co-simulation algorithm. Nat Resour Res 28(1):109–124. https://doi.org/10.1007/s11053-018-9378-3

Habib MA, Islam ARMT, Bodrud-Doza M, Mukta FA, Khan R, Siddique MAB, Phoungthong K, Techato K (2020) Simultaneous appraisals of pathway and probable health risk associated with trace metals contamination in groundwater from Barapukuria coal basin, Bangladesh. Chemosphere 242:125183. https://doi.org/10.1016/j.chemosphere.2019.125183

Haghshenas V, Kafaei R, Tahmasebi R, Dobaradaran S, Hashemi S, Sahebi S, Sorial GA, Ramavandi B (2019) Potential of green/brown algae for monitoring of metal(loid)s pollution in the coastal seawater and sediments of the Persian Gulf: ecological and health risk assessment. Environ Sci Pollut R 27:7463–7475. https://doi.org/10.1007/s11356-019-07481-0

Haris H, Looi LJ, Aris AZ, Mokhtar NF, Ayob NAA, Yusoff FM, Salleh A, Praveena SM (2017) Geo-accumulation index and contamination factors of heavy metals (Zn and Pb) in urban river sediment. Environ Geochem Hlth 39(6):1259–1271. https://doi.org/10.1007/s10653-017-9971-0

Harris MJ, Stinson J, Landis WG (2017) A bayesian approach to integrated ecological and human health risk assessment for the South River, Virginia mercury-contaminated site. Risk Anal 37(7):1341–1357. https://doi.org/10.1111/risa.12691

Hossain MB, Shanta TB, Ahmed ASS, Hossain MK, Semme SA (2019) Baseline study of heavy metal contamination in the Sangu River estuary, Chattogram, Bangladesh. Mar Pollut Bull 140:255–261. https://doi.org/10.1016/j.marpolbul.2019.01.058

Hosseini NS, Sobhanardakani S, Cheraghi M, Lorestani B, Merrikhpour H (2020) Heavy metal concentrations in roadside plants (Achillea wilhelmsii and Cardaria draba) and soils along some highways in Hamedan, west of Iran. Environ Sci Pollut R 27:13301–13314. https://doi.org/10.1007/s11356-020-07874-6

Islam ARMT, Islam HM, Mia MU, Khan R, Habib MA, Bodrud-Doza M, Siddique MAB, Chu R (2020a) Co-distribution, possible origins, status and potential health risk of trace elements in surface water sources from six major river basins, Bangladesh. Chemosphere 249:126180. https://doi.org/10.1016/j.chemosphere.2020.126180

Islam ARMT, Siddiqua MT, Zahid A, Tasnim SS, Rahman MM (2020b) Drinking appraisal of coastal groundwater in Bangladesh: an approach of multi-hazards towards water security and health safety. Chemosphere 255:126933. https://doi.org/10.1016/j.chemosphere.2020.126933

Javadi S, Hashemy SM, Mohammadi K, Howard KWF, Neshat A (2017) Classification of aquifer vulnerability using K-means cluster analysis. J Hydrol 549:27–37. https://doi.org/10.1016/j.jhydrol.2017.03.060

Keller A, Abbaspour KC, Schulin R (2002) Assessment of uncertainty and risk in modeling regional heavy-metal accumulation in agricultural soils. J Environ Qual 31(1):175–187

Liu C, Liu Y, Feng CL, Wang P, Yu LP, Liu DQ, Sun SH, Wang FK (2021) Distribution characteristics and potential risks of heavy metals and antimicrobial resistant Escherichia coli in dairy farm wastewater in Tai'an, China. Chemosphere 262:127768. https://doi.org/10.1016/j.chemosphere.2020.127768

Lu HW, Li J, Ren LX, Chen YZ (2018) Optimal groundwater security management policies by control of inexact health risks under dual uncertainty in slope factors. Chemosphere 198:161–173. https://doi.org/10.1016/j.chemosphere.2018.01.121

Maere T, Villez K, Marsili-Libelli S, Naessens W, Nopens I (2012) Membrane bioreactor fouling behaviour assessment through principal component analysis and fuzzy clustering. Water Res 46(18):6132–6142. https://doi.org/10.1016/j.watres.2012.08.027

Martinez-Cortijo J, Ruiz-Canales A (2018) Effect of heavy metals on rice irrigated fields with waste water in high pH Mediterranean soils: the particular case of the Valencia area in Spain. Agr Water Manage 210:108–123. https://doi.org/10.1016/j.agwat.2018.07.037

Men C, Liu RM, Xu F, Wang QR, Guo LJ, Shen ZY (2018) Pollution characteristics, risk assessment, and source apportionment of heavy metals in road dust in Beijing, China. Sci Total Environ 612:138–147. https://doi.org/10.1016/j.scitotenv.2017.08.123

Nath BK, Chaliha C, Bhuyan B, Kalita E, Baruah DC, Bhagabati AK (2018) GIS mapping-based impact assessment of groundwater contamination by arsenic and other heavy metal contaminants in the Brahmaputra River valley: a water quality assessment study. J Clean Prod 201:1001–1011. https://doi.org/10.1016/j.jclepro.2018.08.084

Pal D, Maiti SK (2018) Seasonal variation of heavy metals in water, sediment, and highly consumed cultured fish (Labeo rohita and Labeo bata) and potential health risk assessment in aquaculture pond of the coal city, Dhanbad (India). Environ Sci Pollut R 25(13):12464–12480. https://doi.org/10.1007/s11356-018-1424-5

Paschoalini AL, Savassi LA, Arantes FP, Rizzo E, Bazzoli N (2019) Heavy metals accumulation and endocrine disruption in Prochilodus argenteus from a polluted neotropical river. Ecotox

Environ Safe 169:539–550. https://doi.org/10.1016/j.ecoenv.2018.11.047

Peiris RH, Halle C, Budman H, Moresoli C, Peldszus S, Huck PM, Legge RL (2010) Identifying fouling events in a membrane-based drinking water treatment process using principal component analysis of fluorescence excitation-emission matrices. Water Res 44(1):185–194. https://doi.org/10.1016/j.watres.2009.09.036

Ren LX, He L, Lu HW, Chen YZ (2016) Monte Carlo-based interval transformation analysis for multi-criteria decision analysis of groundwater management strategies under uncertain naphthalene concentrations and health risks. J Hydrol 539:468–477. https://doi.org/10.1016/j.jhydrol.2016.05.063

Saha N, Rahman MS, Ahmed MB, Zhou JL, Ngo HH, Guo WS (2017) Industrial metal pollution in water and probabilistic assessment of human health risk. J Environ Manag 185:70–78. https://doi.org/10.1016/j.jenvman.2016.10.023

Shabanda IS, Koki IB, Low KH, Zain SM, Khor SM, Abu Bakar NK (2019) Daily exposure to toxic metals through urban road dust from industrial, commercial, heavy traffic, and residential areas in Petaling Jaya, Malaysia: a health risk assessment. Environ Sci Pollut R 26(36):37193–37211. https://doi.org/10.1007/s11356-019-06718-2

Sharafi K, Nodehi RN, Yunesian M, Mahvi AH, Pirsaheb M, Nazmara S (2019) Human health risk assessment for some toxic metals in widely consumed rice brands (domestic and imported) in Tehran, Iran: uncertainty and sensitivity analysis. Food Chem 277:145–155. https://doi.org/10.1016/j.foodchem.2018.10.090

Singh UK, Kumar B (2017) Pathways of heavy metals contamination and associated human health risk in Ajay River basin, India. Chemosphere 174:183–199. https://doi.org/10.1016/j.chemosphere.2017.01.103

Swain R, Sahoo B (2017) Mapping of heavy metal pollution in river water at daily time-scale using spatio-temporal fusion of MODIS-aqua and Landsat satellite imageries. J Environ Manag 192:1–14. https://doi.org/10.1016/j.jenvman.2017.01.034

Tepanosyan G, Sahakyan L, Belyaeva O, Asmaryan S, Saghatelyan A (2018) Continuous impact of mining activities on soil heavy metals levels and human health. Sci Total Environ 639:900–909. https://doi.org/10.1016/j.scitotenv.2018.05.211

Troldborg M, Duckett D, Allan R, Hastings E, Hough RL (2017) A risk-based approach for developing standards for irrigation with reclaimed water. Water Res 126:372–384. https://doi.org/10.1016/j.watres.2017.09.041

U.S. Environmental Protection Agency Risk Characterization Handbook, Science Policy Council Handbook, EPA 100-B-00-002, 2000

Viswanath NC, Kumar PGD, Ammad KK (2015) Statistical analysis of quality of water in various water shed for Kozhikode City, Kerala, India. Aquatic Procedia 4:1078–1085. https://doi.org/10.1016/j.aqpro.2015.02.136

Wang XY, Xu HZ, Zhou YD, Wu CW, Kanchanopas-Barnette P (2015) Distribution and source apportionment of polycyclic aromatic hydrocarbons in surface sediments from Zhoushan Archipelago and Xiangshan Harbor, East China Sea. Mar Pollut Bull 101(2):895–902. https://doi.org/10.1016/j.marpolbul.2015.10.073

Withanachchi SS, Ghambashidze G, Kunchulia I, Urushadze T, Ploeger A (2018) Water quality in surface water: a preliminary assessment of heavy metal contamination of the Mashavera River, Georgia. Int J Env Res Pub He 15(4):621. https://doi.org/10.3390/ijerph15040621

Yu YJ, Liu LT, Chen XC, Xiang MD, Li ZR, Liu Y, Zeng Y, Han YJ, Yu ZL (2021) Brominated flame retardants and heavy metals in common aquatic products from the Pearl River Delta, South China: bioaccessibility assessment and human health implications. J Hazard Mater 403:124036. https://doi.org/10.1016/j.jhazmat.2020.124036

Zafra C, Temprano J, Suarez J (2017) A simplified method for determining potential heavy metal loads washed-off by stormwater runoff from road-deposited sediments. Sci Total Environ 601:260–270. https://doi.org/10.1016/j.scitotenv.2017.05.178

Zhang YN, Chu CL, Li T, Xu SG, Liu L, Ju MT (2017) A water quality management strategy for regionally protected water through health risk assessment and spatial distribution of heavy metal pollution in 3 marine reserves. Sci Total Environ 599:721–731. https://doi.org/10.1016/j.scitotenv2017.04.232

Zivkovic N, Takic L, Djordjevic L, Djordjevic A, Mladenovic-Ranisavljevic I, Golubovic T, Bozilov A (2019) Pol J Environ Stud 28(3): 2009-2020. https://doi.org/10.15244/pjoes/89986